c. 2

NACA

RESEARCH MEMORANDUM

THE CALCULATION OF THE PATH OF A JETTISONABLE NOSE SECTION

By Roscoe H. Goodwin

Langley Aeronautical Laboratory
Langley Air Force Base, Va.

NATIONAL ADVISORY COMMITTEE
FOR AERONAUTICS

WASHINGTON

September 7, 1950

NATIONAL ADVISORY COMMITTEE FOR AERONAUTICS

RESEARCH MEMORANDUM

THE CALCULATION OF THE PATH OF A JETTISONABLE NOSE SECTION

By Roscoe H. Goodwin

SUMMARY

A method is presented for calculating the path of a jettisonable nose section at any speed by means of successive approximations (solved graphically) using static aerodynamic characteristics. A comparison is made of paths calculated by this method with paths determined experimentally at low speeds. In addition, the paths that a fin-stabilized nose section would follow when jettisoned by various size rockets are calculated for two hypothetical subsonic flight conditions. The minimum size of rocket for successful jettisoning is found and it is shown that a larger size rocket having a shorter duration could also be used.

INTRODUCTION

One of the problems confronting designers of high-speed aircraft is safe pilot escape in an emergency. The conventional bail-out procedure of the past has become more hazardous as the speed of airplanes has increased. Forcible ejection of the pilot in his seat appears to be adequate up to high subsonic speeds. At higher speeds some form of ejection capsule will probably be necessary for pilot escape and one such method is to jettison the nose section of the airplane in which the pilot is seated.

The free-flight stability of typical jettisonable nose sections has been experimentally determined at both low and high speeds as described in references 1, 2, and 3. It has been shown in these investigations that fin stabilization of jettisonable nose sections will prevent their turning away from a nose-first flight attitude and thus will avoid subjecting the pilot to large accelerations. The problem of separating the nose from the rest of the airplane has also been considered, and an experimental study for one design is indicated in reference 3. While dynamic tests, such as those of reference 3, could be made on each proposed design to determine the relative motions of the nose and the

rest of the airplane, they would have to be made for many flight conditions and the whole test program repeated for each means of jettisoning to be considered. A method of successive approximations has been applied herein to the problem of calculating the paths of a jettisonable nose section at any speed through use of static aerodynamic data. As a check on this method, comparisons are presented between low-speed experimental results of reference 3 and calculations made by the subject method for the same conditions and using the low-speed aerodynamic data of reference 4. Also, calculations of the path of a fin-stabilized nose section when jettisoned by rocket propulsion for two initial subsonic flight conditions are presented.

SYMBOLS

X	longitudinal reference axis, coincident at instant of jettisoning to longitudinal body axis of airplane (See fig. 1.)
Z	normal reference axis, parallel at instant of jettisoning to normal body axis of airplane (See fig. 1.)
F_X	total force parallel to X-axis, pounds
F_Z	total force parallel to Z-axis, pounds
s_X	separation of nose section from rest of airplane, measured parallel to X-axis, feet
s_Z	separation of nose section from rest of airplane, measured parallel to Z-axis, feet
V_X	velocity of nose section relative to rest of airplane along X-axis, feet per second
V_Z	velocity of nose section relative to rest of airplane along Z-axis, feet per second
V_p	resultant velocity of airplane at instant of jettisoning, feet per second
V_{X_p}	component along X-axis of velocity of airplane at instant of jettisoning, feet per second
V_{Z_p}	component along Z-axis of velocity of airplane at instant of jettisoning, feet per second

[redacted]

V_R	resultant airspeed of nose section, feet per second
ω	angular velocity of nose in pitch, radians per second
C_L	lift coefficient of nose section (L/qS)
C_D	drag coefficient of nose section (D/qS)
C_M	pitching-moment coefficient of nose section $(M/qS\bar{c})$
L	lift of nose section, pounds
D	drag of nose section, pounds
M	pitching moment of nose section about its center of gravity, foot-pounds
ρ	air density, slugs per cubic foot
g	acceleration due to gravity, feet per second per second
S	wing area of airplane, square feet
$\bar{c}$	mean aerodynamic chord of airplane wing, feet
q	dynamic pressure, pounds per square foot, $\left(\frac{1}{2}\rho V_R^2\right)$
I	pitching moment of inertia of nose section about its center of gravity, slug-feet squared
m	mass of nose section, slugs
t	time, measured from instant of jettisoning, seconds
Δt	interval of time between consecutive calculated points
T	thrust of ejection rockets (or pistons), pounds
W	weight of nose section, pounds
α	angle of attack of nose section, degrees
α_p	angle of attack of airplane at instant of jettisoning, degrees
γ	flight-path angle of airplane at instant of jettisoning, degrees
θ	angle between axis of symmetry of nose section and X-axis, degrees

[redacted]

π angle that relative wind on nose makes with X-axis, degrees

σ angle between thrust line of ejection rockets (or pistons) and X-axis, degrees

ϕ angle between axis of symmetry of nose section and thrust line of ejection rockets (or pistons), degrees

ψ angle between X-axis and the horizontal, degrees

d diameter of base of nose section, feet

r radius of base of nose section, feet

l distance between thrust line of rocket and center of gravity, measured perpendicular to rocket thrust line, feet

Ap acceleration along backbone of pilot, g units

F_p total force along backbone of pilot, pounds

Subscripts:

X X-axis

Z Z-axis

p airplane

P pilot

R resultant

METHOD AND ANALYSIS

DESCRIPTION OF THE METHOD USED

Since the path that a jettisoned nose follows relative to the rest of the airplane and the aerodynamic forces and moments on the nose are interdependent, no direct method can be used for calculating the path. A method of successive approximations utilizing graphical integration has been set up and is described herein.

Since the aerodynamic data in reference 4 are plotted against separation along the body axes of the airplane, these axes are used as

the reference axes for the derivation of all the equations. Because the variation of the aerodynamic characteristics of the airplane with nose separation is not known, the rest of the airplane is assumed to hold its original course and speed during separation. The error due to this assumption should be small due to the large inertia of the rest of the airplane and the small period of time covered by these calculations. The main effects on the airplane of jettisoning the nose section should be an increase in drag and a rearward shift of its center of gravity, both of which will aid the separation so that the present calculations, in neglecting them, should be conservative.

From figure 1 the total force exerted on the nose section parallel to the X-axis is

$$F_X = T \cos \sigma - W \sin \psi - D \cos \pi + L \sin \pi \tag{1}$$

the total force parallel to the Z-axis is

$$F_Z = T \sin \sigma + W \cos \psi - D \sin \pi - L \cos \pi \tag{2}$$

and the total pitching moment is

$$M_R = M + Tl \tag{3}$$

The velocities imparted to the nose section by these forces and moments can be calculated from the following relations:

$$V_X = \frac{1}{m} \int F_X \, dt \tag{4}$$

$$V_Z = \frac{1}{m} \int F_Z \, dt \tag{5}$$

$$\omega = \frac{1}{I} \int M_R \, dt \tag{6}$$

These equations can easily be solved by plotting curves of the variations of F_X, F_Z, and M_R with time and integrating graphically. The variation

[redacted]

of displacement with time can be found from the equations

$$s_X = \int V_X \, dt \tag{7}$$

$$s_Z = \int V_Z \, dt \tag{8}$$

$$\theta = 57.3 \int \omega \, dt \tag{9}$$

These equations may be solved by graphical integration of curves of V_X, V_Z, and ω against t.

The angle π that the relative wind makes with the X-axis at any time is

$$\pi = \tan^{-1} \frac{V_Z + V_{Z_p}}{V_X + V_{X_p}} \tag{10}$$

where

$$V_{X_p} = V_p \cos \alpha_p \tag{11}$$

and

$$V_{Z_p} = V_p \sin \alpha_p \tag{12}$$

The angle of attack of the nose section at any time can be found from the relation

$$\alpha = \pi + \theta \tag{13}$$

From equations (7), (8), and (13), values of s_X, s_Z, and α at various times are known, and C_L, C_D, and C_M can be found from aerodynamic data for the nose section under consideration. Lift, drag, and pitching moment may be calculated from the equations

$$L = C_L \frac{\rho}{2} S V_R^2 \tag{14}$$

$$D = C_D \frac{\rho}{2} S V_R^2 \tag{15}$$

[redacted]

$$M = C_M \frac{\rho}{2} S \bar{c} V_R^2 \tag{16}$$

where

$$V_R^2 = \left(V_X + V_{X_p}\right)^2 + \left(V_Z + V_{Z_p}\right)^2 \tag{17}$$

From the following equation σ can be found:

$$\sigma = \phi - \theta \tag{18}$$

Equations (10), (14), (15), (16), and (18), together with the constants of the flight condition under consideration, provide all the quantities necessary to solve equations (1), (2), and (3).

To solve a problem using this method, the unknown quantities of equations (1), (2), and (3) are given assumed variations with time, and F_X, F_Z, and M_R are calculated for various values of t. The foregoing procedure (outlined in equations (4) to (18)) is followed and the applicable results are used in equations (1), (2), and (3) as the next approximation. This whole process is repeated until the calculated forces and moments agree with those of the last approximation. A sample calculation illustrating the application of these equations is presented in the appendix.

For the special case of simple release (no propulsive force), the nose will slide down the front of the fuselage and, assuming negligible sliding friction, equations (1) and (2) become

$$F_X = -W \sin \psi - D \cos \pi + L \sin \pi$$

$$F_Z = W \cos \psi - D \sin \pi - L \cos \pi$$

Equation (3) is replaced by the following two alternate equations. The total moment M_B about point B is (from fig. 2)

$$M_B = M + rF_X$$

And the total moment M_C about point C is

$$M_C = M - \left(r - s_Z\right)F_X$$

For each value of t, the equation for M_B should be solved first. If M_B is positive, the nose will pitch up, and M_B must be plotted on the curve of the pitching moment against time. If M_B is negative, the equation for M_C should be solved. If M_C is then positive, the nose can pitch neither up nor down, and therefore zero should be plotted on the curve of the pitching moment against time. If M_C is negative, the nose will pitch downward, and M_C must be plotted on the curve of the pitching moment against time. After the nose section clears the remainder of the airplane, equation (3) applies.

Since the objective in this work is to jettison the nose section without injuring the pilot, the various paths followed by the jettisoned nose section must be examined for the accelerations they impose on the pilot. The critical accelerations are those acting along the backbone of the pilot and causing him to "blackout" or "redout," depending upon the sense of the force. The acceleration experienced by the pilot (fig. 3), if the small component due to acceleration in pitch is neglected, is

$$A_P = \frac{-F_P}{W} \tag{19}$$

where

$$F_P = F_Z \cos\theta + F_X \sin\theta \tag{20}$$

Therefore,

$$A_P = \frac{-F_Z \cos\theta - F_X \sin\theta}{W} \tag{21}$$

The signs of equation (21) are such that A_P will follow the aeromedical sign convention; that is, negative acceleration is acceleration tending to make blood rush toward the head.

[redacted]

COMPARISON WITH EXPERIMENTAL DATA

In order to check the present method against experimentally determined results, the path that the nose follows during jettisoning was calculated by using low-speed aerodynamic data from reference 4 for conditions corresponding to two of the test runs of reference 3. In these test runs the tunnel airspeed was 125 miles per hour. The nose was released with and without stabilizing fins from the airplane model which was at 0° angle of attack. The results of these calculations are compared with the data from reference 3 in figures 4 to 9 as plots of displacements and accelerations of the full-scale airplane nose section against time. In general, there is close agreement between the curves. Since the nose without stabilizing fins attached turned away from a nose-first attitude after leaving the fuselage (reference 3), it was impossible to calculate the rest of the path inasmuch as the data of reference 4 are only for angles of attack of 0° and 5°. When data are available for higher angles of attack, the present method can be applied to an unfinned nose if the dynamic derivatives are considered negligible.

The major discrepancies between the calculated and experimental curves are in the time scales. It is felt that these discrepancies could be attributed to the fact that zero time was originally established in reference 3 as the time of the motion-picture frame preceding that in which movement of the nose was first detected, and, since the initial velocity of the nose section is small, it is quite possible that movement during the first 0.05 second (the full-scale time between frames) could have passed unnoticed on the film. In transferring the vertical-acceleration curves from reference 3, the signs were changed, inasmuch as the aeromedical sign convention, which was used in reference 3, is based on the reaction of the blood in the body.

THE PATH OF A ROCKET-JETTISONED NOSE SECTION

Conditions

The path that the nose section of reference 4, with stabilizing fins attached, would take if jettisoned from an airplane by means of rocket propulsion has been calculated for four different amounts of rocket thrust. For the two largest rockets, the effect on the path of

shortening the duration of thrust was calculated, and for the smallest rocket, the effect of a lower initial velocity of the airplane was calculated. For all the calculations, the following constants were assumed:

ρ = 0.001496 slug per cubic foot (15,000-ft altitude)

S = 175 square feet

V_p = 800 feet per second

V_p (alternate) = 700 feet per second

$\bar{c}$ = 7.27 feet

d = 4.4 feet

W = 815 pounds

m = 25.3 slugs

I = 90.5 slug-feet squared

$\alpha_p = 2^\circ$

$\gamma = -5^\circ$

$\phi = 26^\circ$

Δt = 0.02 second

The distance l was selected in each case to keep the nose section within the range of angle of attack of reference 4 throughout the computations, and its magnitude is indicated in the figures presenting the various paths.

Results and Discussion

The paths of the fin-stabilized nose section, jettisoned at 800 feet per second, with various rocket thrusts are presented in figure 10. For these calculations, the rockets were assumed to have a duration sufficient to carry the nose section out of the area for which the aerodynamic characteristics are known. The accelerations along the pilot's backbone for each of these paths are shown in figure 11. Whereas a rocket having a 2800-pound thrust, which lasts until the nose section is below the main fuselage, would seem to be the minimum size to ensure continued separation as shown in figure 10, another approach to the problem would be to use a more powerful rocket of shorter duration. The most powerful

rocket used for the paths shown in figure 10 (4300-pound thrust) was assumed to have durations of 0.16 second and 0.20 second and the resulting paths were calculated. These paths are presented in figure 12 along with the original path for this rocket assuming a duration of 0.30 second, and the accelerations on the pilot are shown in figure 13. The next most powerful rocket (3600-pound thrust) was assumed to have a duration of 0.20 second and the path of the nose section using this rocket was calculated. This path and the accelerations it imposes on the pilot are shown in figures 14 and 15, respectively, with the results of an assumed duration of 0.32 second repeated for comparison. Use of a large rocket of short duration is shown to be possible, but, unless the duration can be very accurately controlled, it would not seem advisable inasmuch as a change of 0.04 second can spell the difference between collision of the nose section and the rest of the airplane or clearance by a wide margin (fig. 12). Finally, the effect of reducing the initial velocity on the path of the nose section using the 2800-pound rocket was calculated. The paths for 800 feet per second and 700 feet per second are compared in figure 16 and the accelerations, in figure 17.

In order to evaluate the paths shown in figures 10, 12, 14, and 16, it is necessary to know what value s_Z must have to prevent collision of the nose section with the rest of the airplane when s_X again becomes zero. Two front-view drawings are presented in figure 18 and show the minimum vertical displacement (s_Z) necessary to prevent collision of the nose and the rest of the airplane. Placing the fins in the 45° planes (fig. 18) would reduce the value of s_Z required for successful jettisoning, and, since the investigation of reference 4 found negligible difference between the aerodynamic characteristics of the nose for the alternate fin locations, it would not change the path followed by the nose section.

If the time interval chosen in applying the present method is small enough, the faired curves of force, moment, and velocity will represent the actual variations with time and the true path of the nose section under consideration will be found. In order to check on the time interval of 0.02 second chosen for the present calculations, the path of the nose section jettisoned with the 2800-pound rocket was also calculated by use of a time interval of 0.01 second. The results of these calculations are included in figure 16 (only odd-numbered time intervals are plotted), and the close agreement of the two paths would seem to indicate that a time interval of 0.02 second is sufficiently small for the conditions calculated in this paper.

CONCLUDING REMARKS

A method has been outlined whereby the path of a jettisonable nose section at any speed may be calculated from the instant of its release, assuming that its static aerodynamic characteristics be known. The effects of different jettisoning forces on the path of a typical fin-stabilized nose section have been shown for one set of initial subsonic conditions, and the change in path due to reducing the intitial velocity for one case has also been shown. The minimum practicable jettisoning force for the given set of conditions was found, and it was shown that a larger force acting for a shorter time would be satisfactory although the duration would be quite critical.

Langley Aeronautical Laboratory
National Advisory Committee for Aeronautics
Langley Air Force Base, Va.

[redacted]

APPENDIX

SAMPLE CALCULATION

The application of the subject method consists of making an assumption of the variation of force and moment with time for a short period and then working through the necessary calculations. The resulting calculated values of F_X, F_Z, and M_R are plotted against time and the curves are extended by further assumptions. The calculations are again carried out for values of t beyond that value at which the assumed and calculated curves do no longer coincide.

As a numerical example, the formulas are solved for the 2800-pound rocket thrust at $t = 0.18$ second. The numbers in parentheses after each formula refer to the number of that formula in the text of the report with the letter "a" to denote appendix.

The values of F_X, F_Z, and M_R at $t = 0.18$ second are assumed to be -530 pounds, 4300 pounds, and 1500 foot-pounds, respectively, and are plotted on their respective curves. Graphical integration of the curves yields

$$V_X = \frac{1}{25.3}\int_{t=0}^{t=0.18} F_X \, dt = 4.44 \text{ fps} \qquad (4a)$$

$$V_Z = \frac{1}{25.3}\int_{t=0}^{t=0.18} F_Z \, dt = 17.73 \text{ fps} \qquad (5a)$$

$$\omega = \frac{1}{90.5}\int_{t=0}^{t=0.18} M_R \, dt = -0.444 \text{ radian/sec} \qquad (6a)$$

[redacted]

These values, along with the others for this approximation, are plotted on velocity-time curves and the curves are faired. Graphical integrations of these curves determine S_X, S_Z, and θ as:

$$S_X = \int_{t=0}^{t=0.18} V_X \, dt = 0.57 \text{ ft} \tag{7a}$$

$$S_Z = \int_{t=0}^{t=0.18} V_Z \, dt = 1.21 \text{ ft} \tag{8a}$$

$$\theta = 5.73 \int_{t=0}^{t=0.18} \omega \, dt = -6.54^\circ = -6^\circ \, 32' \tag{9a}$$

Then

$$\pi = \tan^{-1} \frac{V_Z + V_{Z_p}}{V_X + V_{X_p}} = \tan^{-1} \frac{17.73 + 27.9}{4.44 + 800} = \tan^{-1} 0.0567 = 3^\circ \, 15' \tag{10a}$$

and

$$\alpha = \pi + \theta = 3^\circ \, 15' - 6^\circ \, 32' = -3^\circ \, 17' \tag{13a}$$

In order to use the data of reference 4, the separations must be expressed in terms of diameters as

$$\frac{S_X}{d} = \frac{0.57}{4.4} = 0.130$$

$$\frac{S_Z}{d} = \frac{1.21}{4.4} = 0.275$$

[redacted]

With the separations and the angle of attack known, the aerodynamic coefficients are found from reference 4 to be

$$C_L = -0.024$$

$$C_D = 0.037$$

$$C_M = 0.0035$$

The resultant velocity of the nose section is

$$V_R^2 = \left(V_X + V_{X_p}\right)^2 + \left(V_Z + V_{Z_p}\right)^2 = (4.44 + 800)^2 + (17.73 + 27.9)^2 = 649\ (10^3)(\text{fps})^2 \qquad (17a)$$

The lift, drag, and pitching moment are

$$L = C_L \frac{\rho}{2} S V_R^2 = -0.024 \frac{0.001496}{2} 175(649)10^3 = -2039 \text{ lb} \qquad (14a)$$

$$D = C_D \frac{\rho}{2} S V_R^2 = 0.037 \frac{0.001496}{2} 175(649)10^3 = 3143 \text{ lb} \qquad (15a)$$

$$M = C_M \frac{\rho}{2} S \bar{c} V_R^2 = 0.0035 \frac{0.001496}{2} 175(7.27)649(10^3) = 2162 \text{ ft-lb} \qquad (16a)$$

The angle between the rocket thrust line and the X-axis is:

$$\sigma = \phi - \theta = 26^\circ - (-6^\circ\ 32') = 32^\circ\ 32' \qquad (18a)$$

Now F_X, F_Z, and M_R can be found as follows:

$$F_X = T \cos \sigma - W \sin \psi - D \cos \pi + L \sin \pi = 2800(0.8431) - 815 (-0.05234) - 3143(0.9984) + (-2039)0.0567 = -850 \text{ lb} \qquad (1a)$$

[redacted]

$$F_Z = T \sin \sigma + W \cos \Psi - D \sin \pi - L \cos \pi = 2800(0.5378) + 815 (0.9986) - 3143(0.0567) - (-2039)0.9984 = 4177 \text{ lb} \quad (2a)$$

$$M_R = M + Tl = 2162 + 2800(-0.20) = 1602 \text{ ft-lb} \quad (3a)$$

These calculated values of F_X, F_Z, and M_R replace the original assumptions and V_X, V_Z, and W are again calculated, and the results are

$$V_X = \frac{1}{25.3}\int_{t=0}^{t=0.18} F_X \, dt = 4.33 \text{ fps} \quad (4a)$$

$$V_Z = \frac{1}{25.3}\int_{t=0}^{t=0.18} F_X \, dt = 17.68 \text{ fps} \quad (5a)$$

$$\omega = \frac{1}{90.5}\int_{t=0}^{t=0.18} M_R \, dt = -0.432 \text{ radian/sec} \quad (6a)$$

The displacements represented by these velocities are

$$S_X = \int_{t=0}^{t=0.18} V_X \, dt = 0.57 \text{ ft} \quad (7a)$$

$$S_Z = \int_{t=0}^{t=0.18} V_Z \, dt = 1.21 \text{ ft} \quad (8a)$$

$$\theta = 57.3\int_{t=0}^{t=0.18} \omega \, dt = -6.54^\circ = -6^\circ 32' \quad (9a)$$

These values agree with those of the last approximation and thus nothing can be gained by further calculations at $t = 0.18$ second.

[redacted]

REFERENCES

1. Gale, Lawrence J.: The Path and Motion of Scale Models of Jettisonable Nose Sections at Supersonic Speeds as Determined from an Investigation in the Langley Free-Flight Apparatus. NACA RM L9J13a, 1950.

2. Scher, Stanley H.: An Empirical Criterion for Fin Stabilizing Jettisonable Nose Sections of Airplanes. NACA RM L9I28, 1949.

3. Scher, Stanley H., and Gale, Lawrence J.: Motion of a Transonic Airplane Nose Section When Jettisoned As Determined from Wind-Tunnel Investigations on a $\frac{1}{25}$-Scale Model. NACA RM L9L08a, 1950.

4. Goodwin, Roscoe H.: Wind-Tunnel Investigation at Low Speed to Determine Aerodynamic Properties of a Jettisonable Nose Section with Circular Cross Section. NACA RM L9J13, 1950.

[redacted]

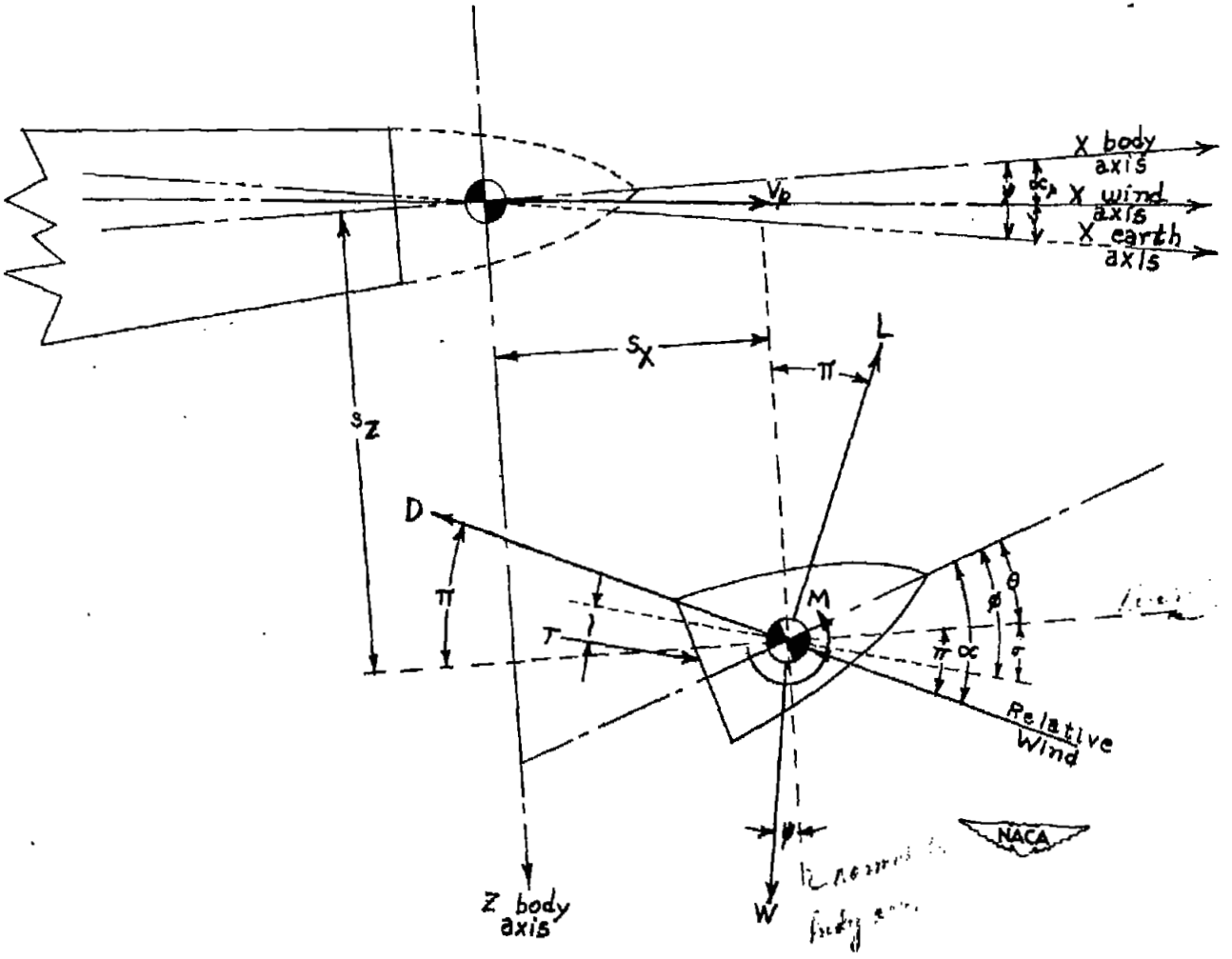

Figure 1.- General sketch of the nose section after jettisoning, showing the positive values of the forces, moments, distances, and angles necessary for the calculation of its path.

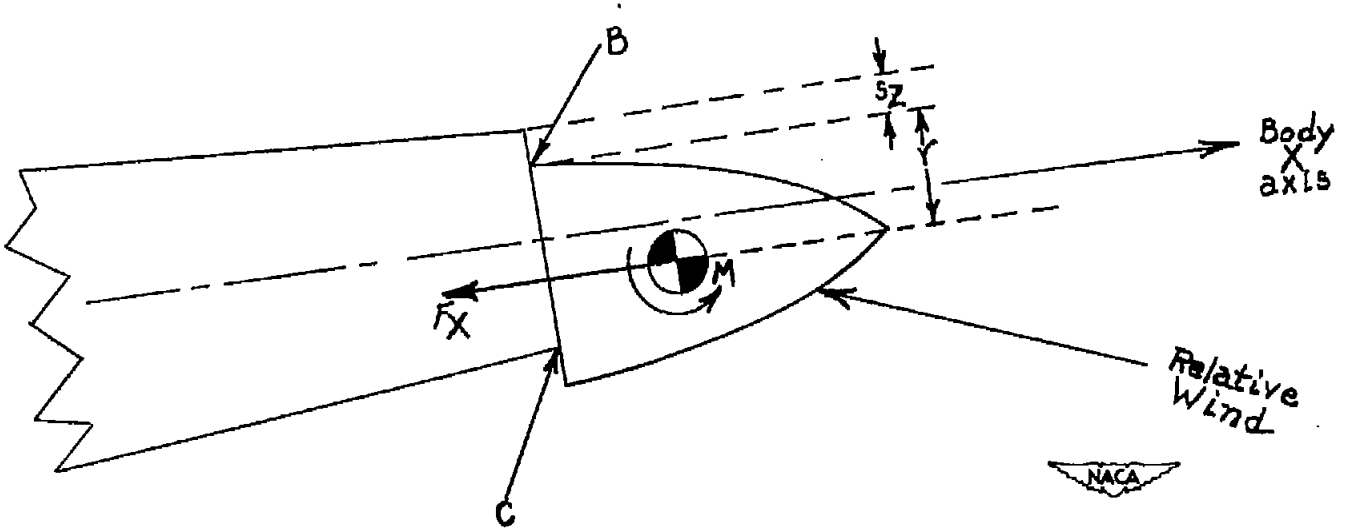

Figure 2.- Sketch showing the information necessary for the determination of the pitching moment of the nose section when no propulsive force is applied. (F_X as shown on the fig. is a negative quantity.)

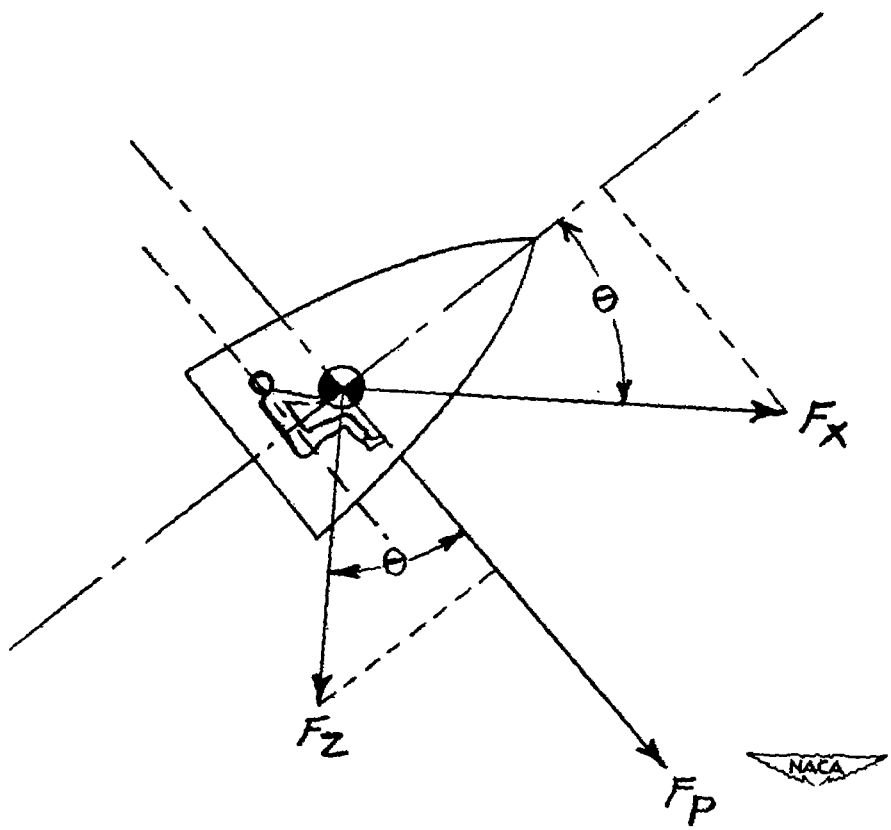

Figure 3.- Sketch showing the information necessary for the determination of the component of acceleration parallel to the backbone of the pilot.

[redacted]

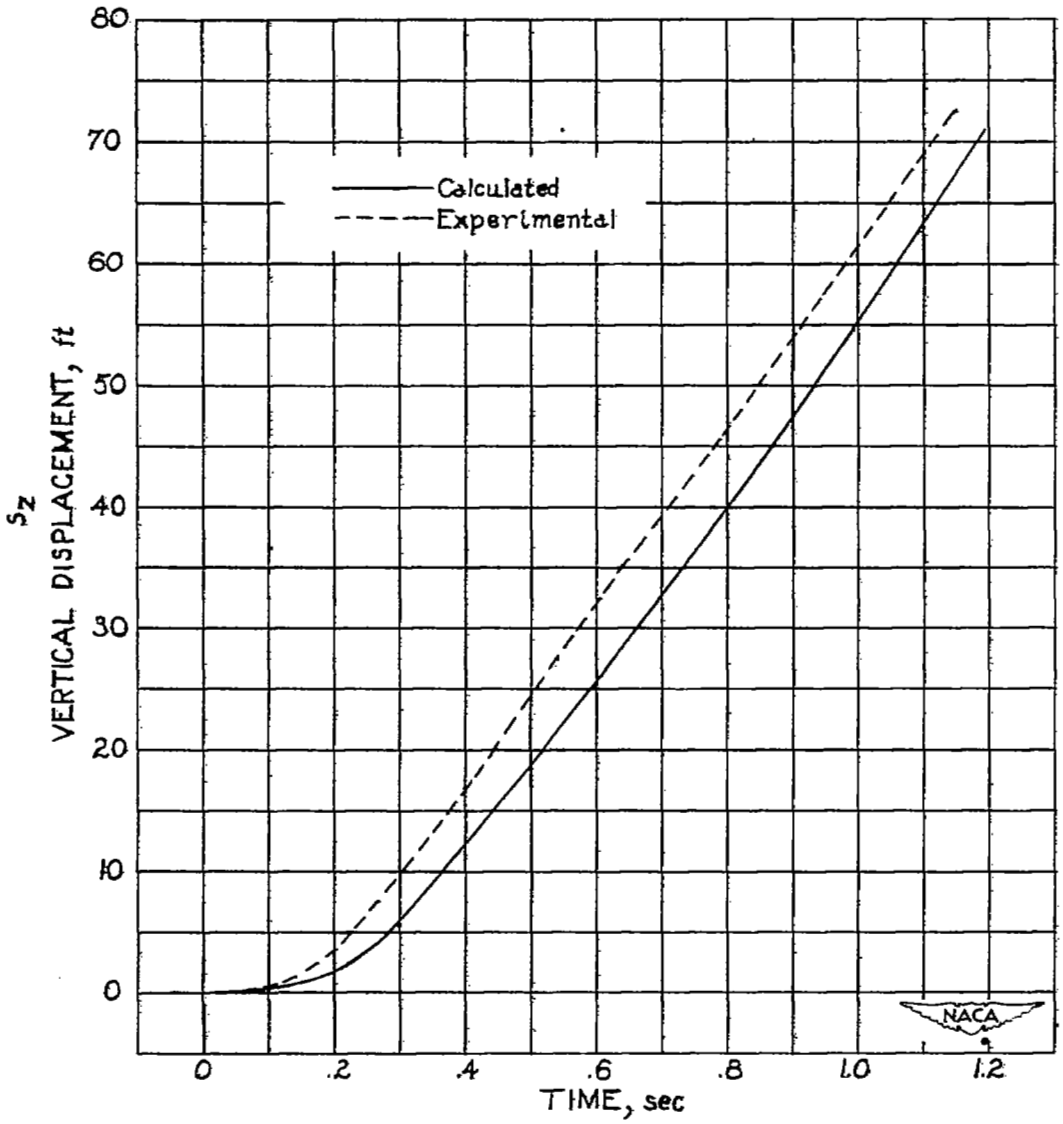

Figure 4.- Comparison of calculated and experimental variations of vertical displacement with time. Stabilizing fins attached to the nose section.

[redacted]

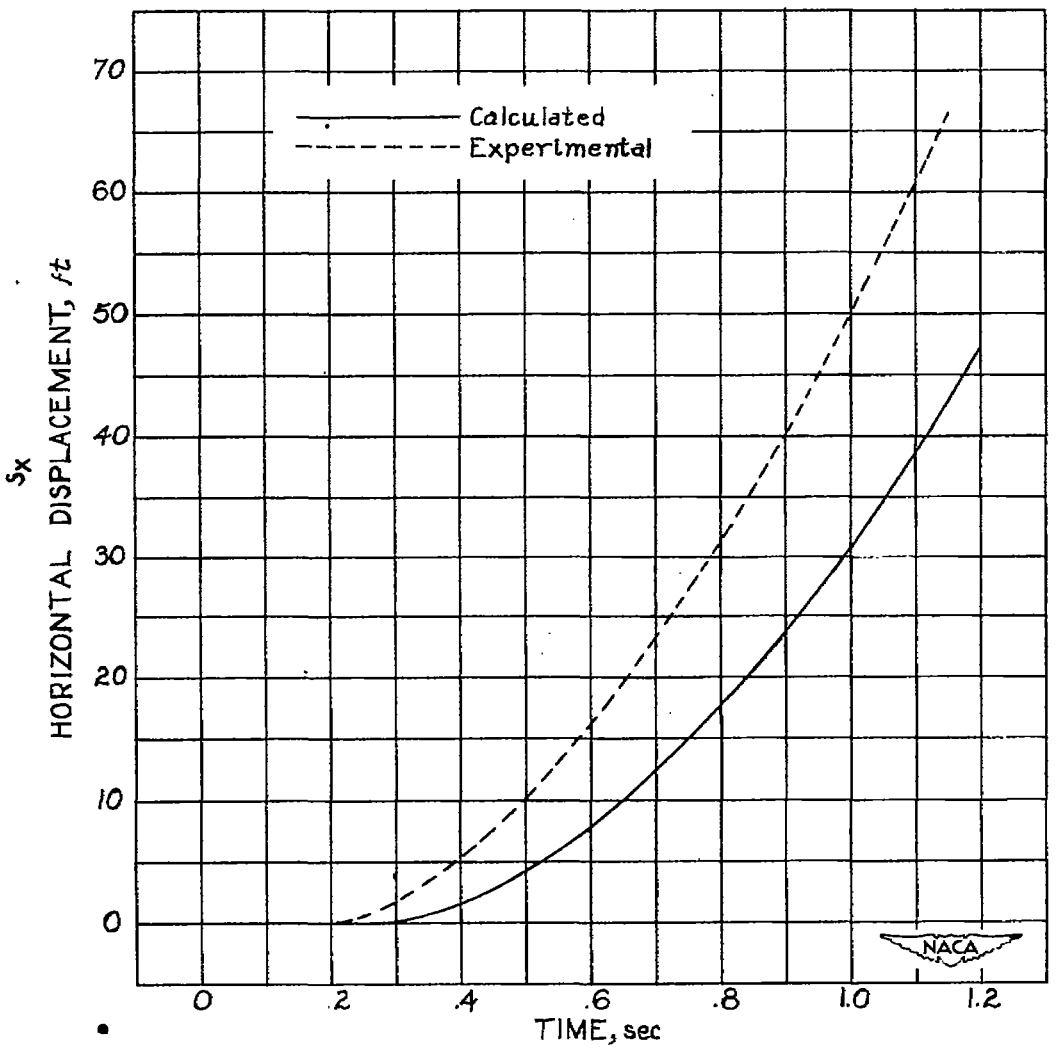

Figure 5.- Comparison of calculated and experimental variations of horizontal displacement with time. Stabilizing fins attached to the nose section.

[redacted]

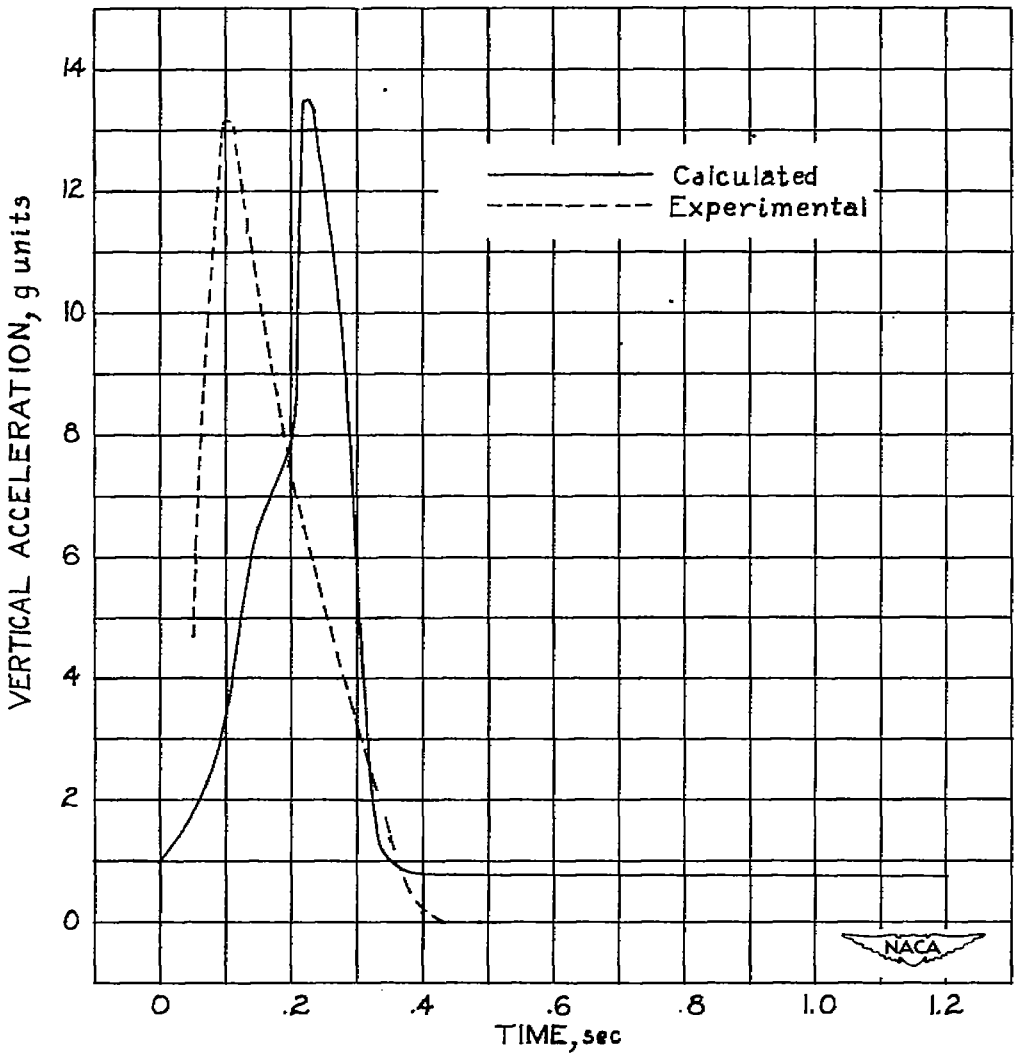

Figure 6.- Comparison of calculated and experimental variations of vertical acceleration with time. Stabilizing fins attached to the nose section.

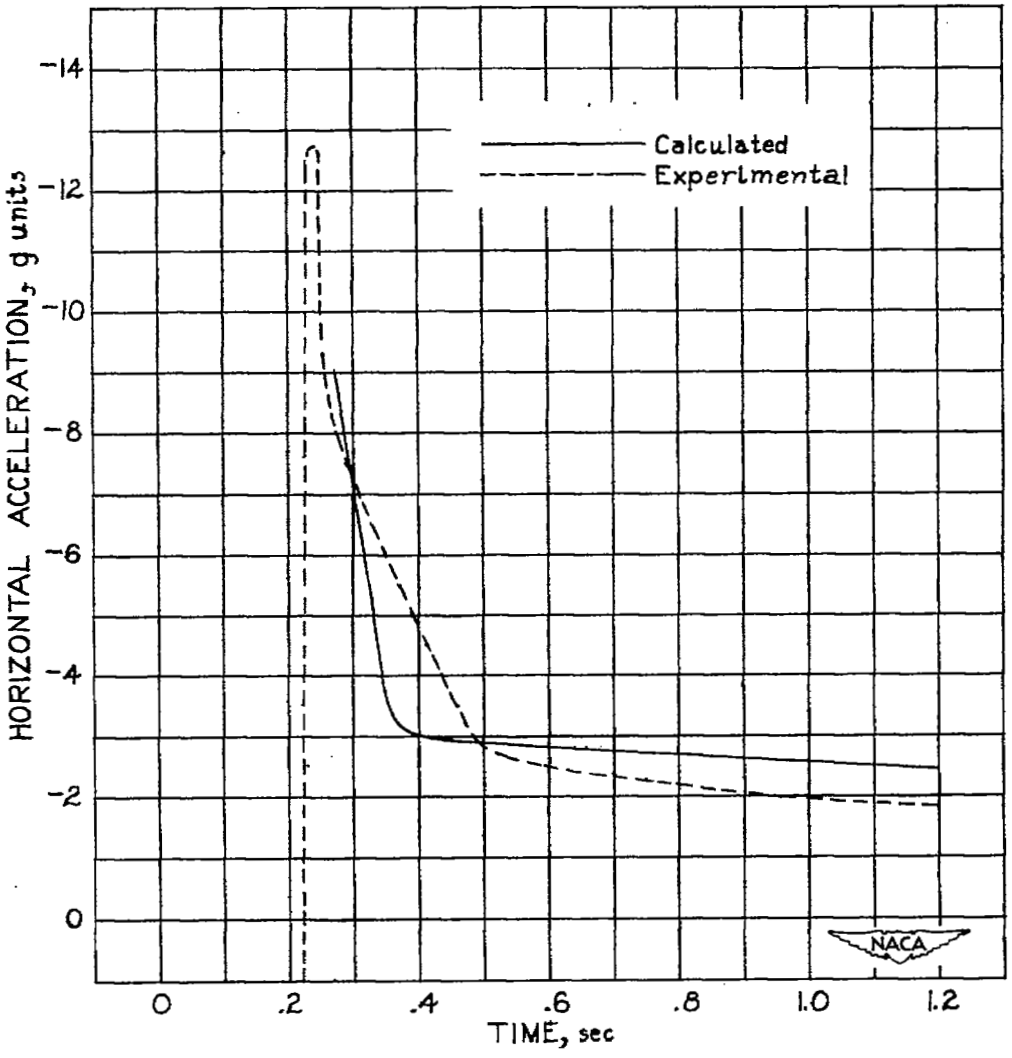

Figure 7.- Comparison of calculated and experimental variations of horizontal acceleration with time. Stabilizing fins attached to the nose section.

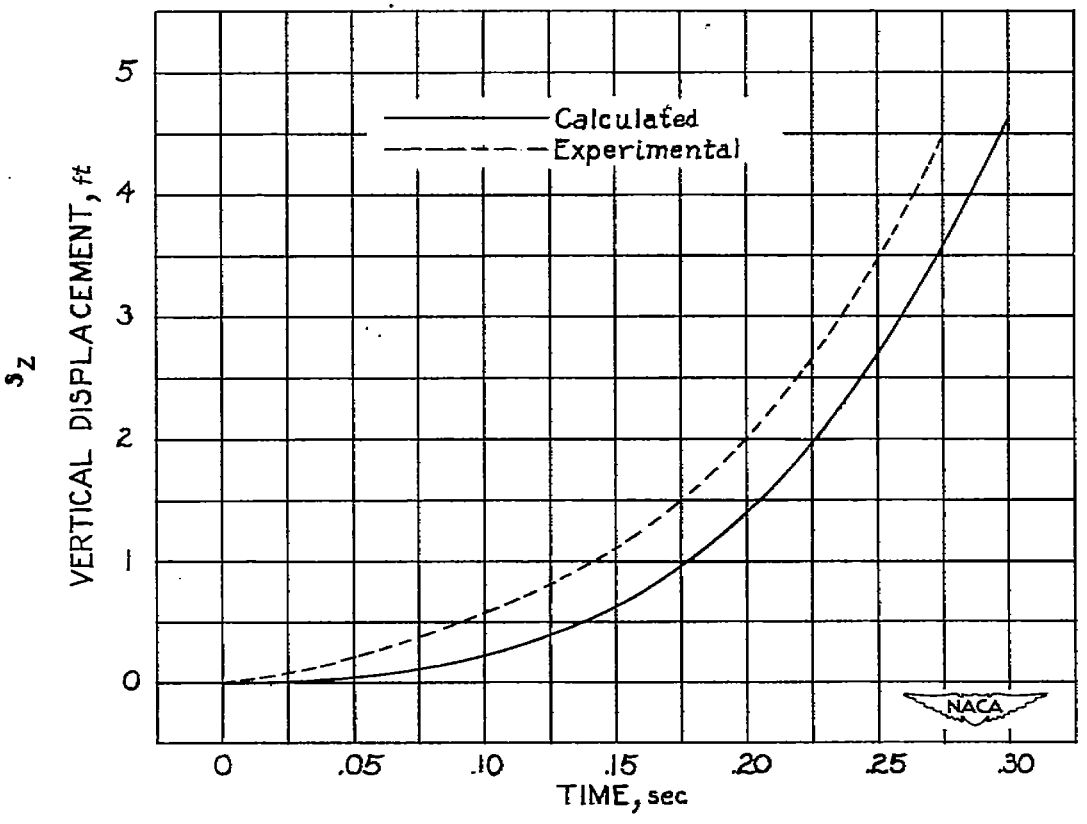

Figure 8.- Comparison of calculated and experimental variations of vertical displacement with time. No stabilizing fins on the nose section.

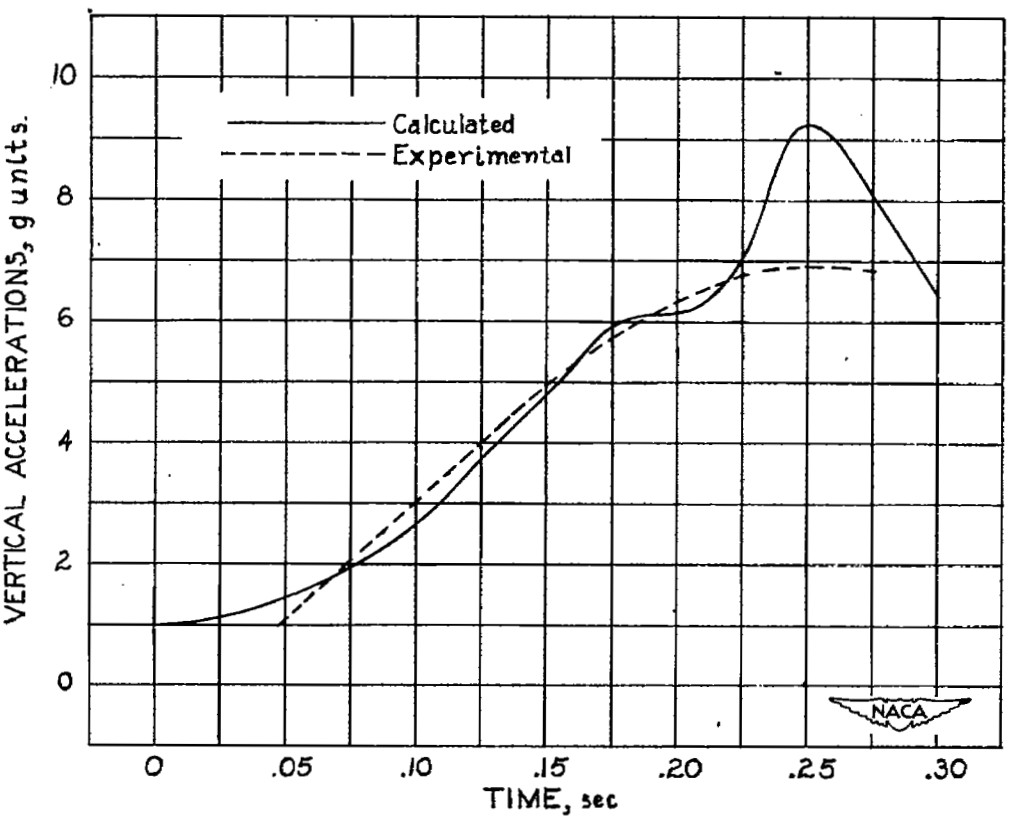

Figure 9.- Comparison of calculated and experimental variations of vertical acceleration with time. No stabilizing fins on the nose section.

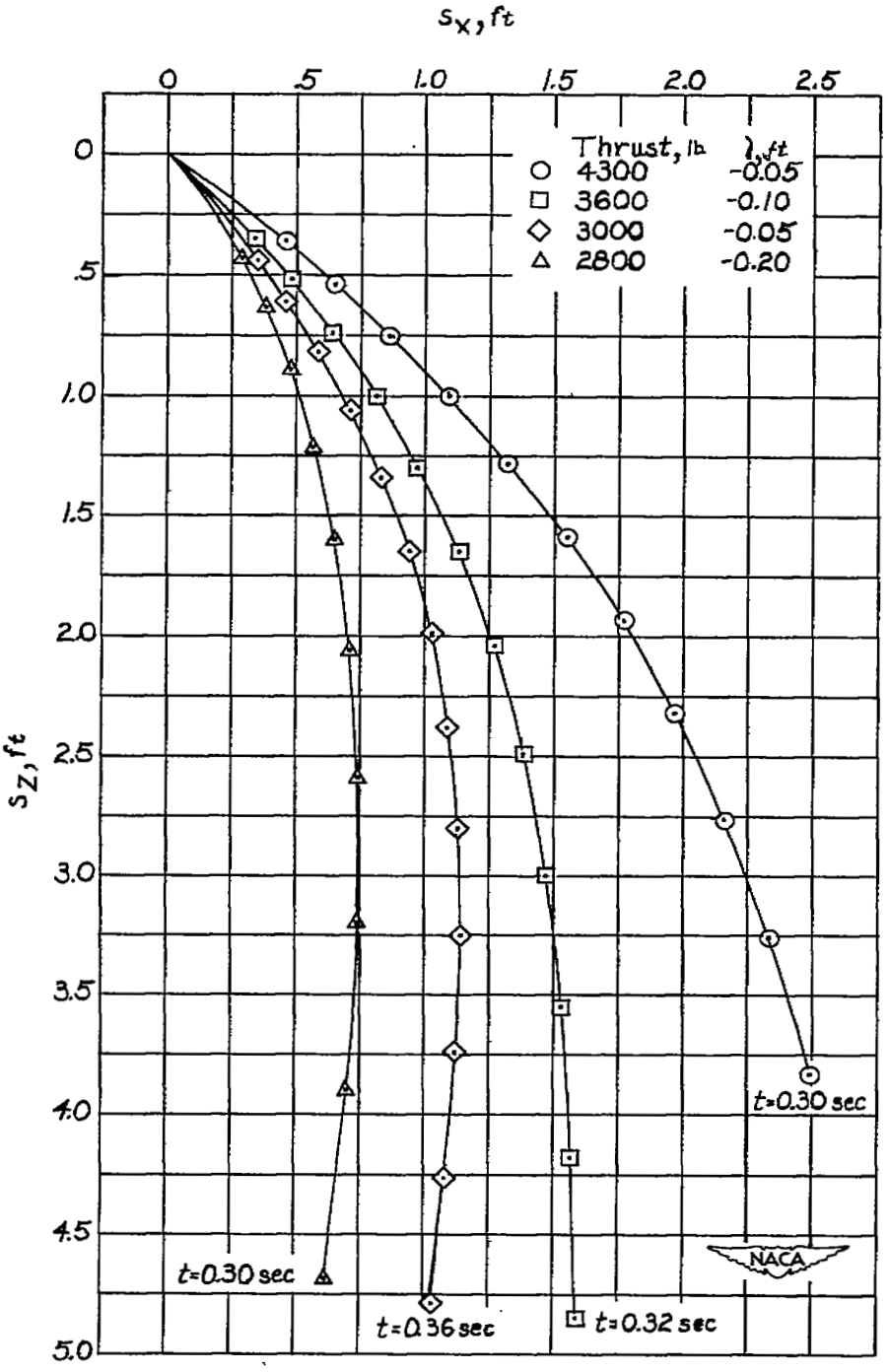

Figure 10.- Paths of the nose section jettisoned by a rocket assuming four different rocket thrusts. V_p = 800 feet per second.

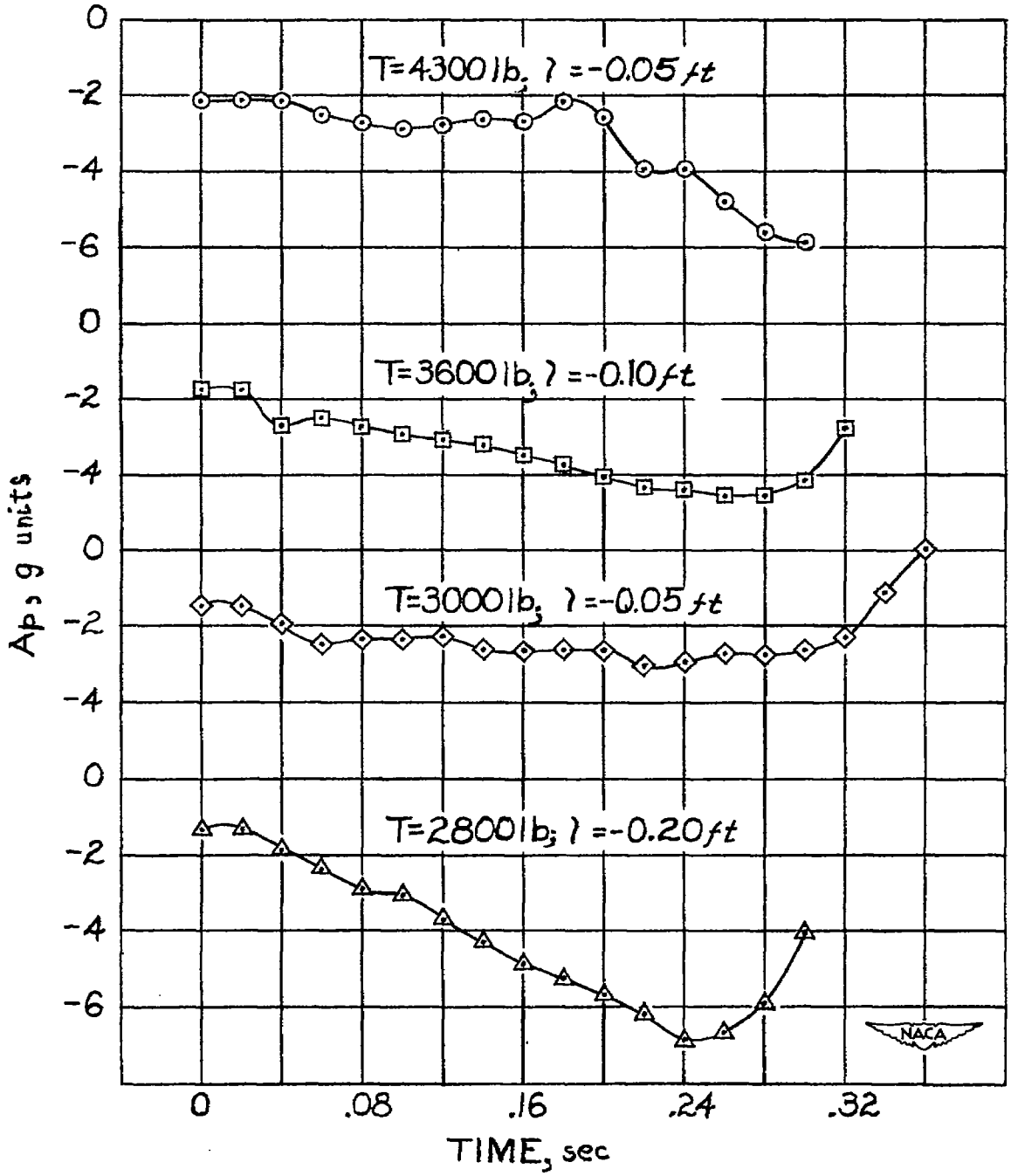

Figure 11.- Accelerations experienced by a pilot within a nose section jettisoned by a rocket assuming four different rocket thrusts. V_p = 800 feet per second.

[redacted]

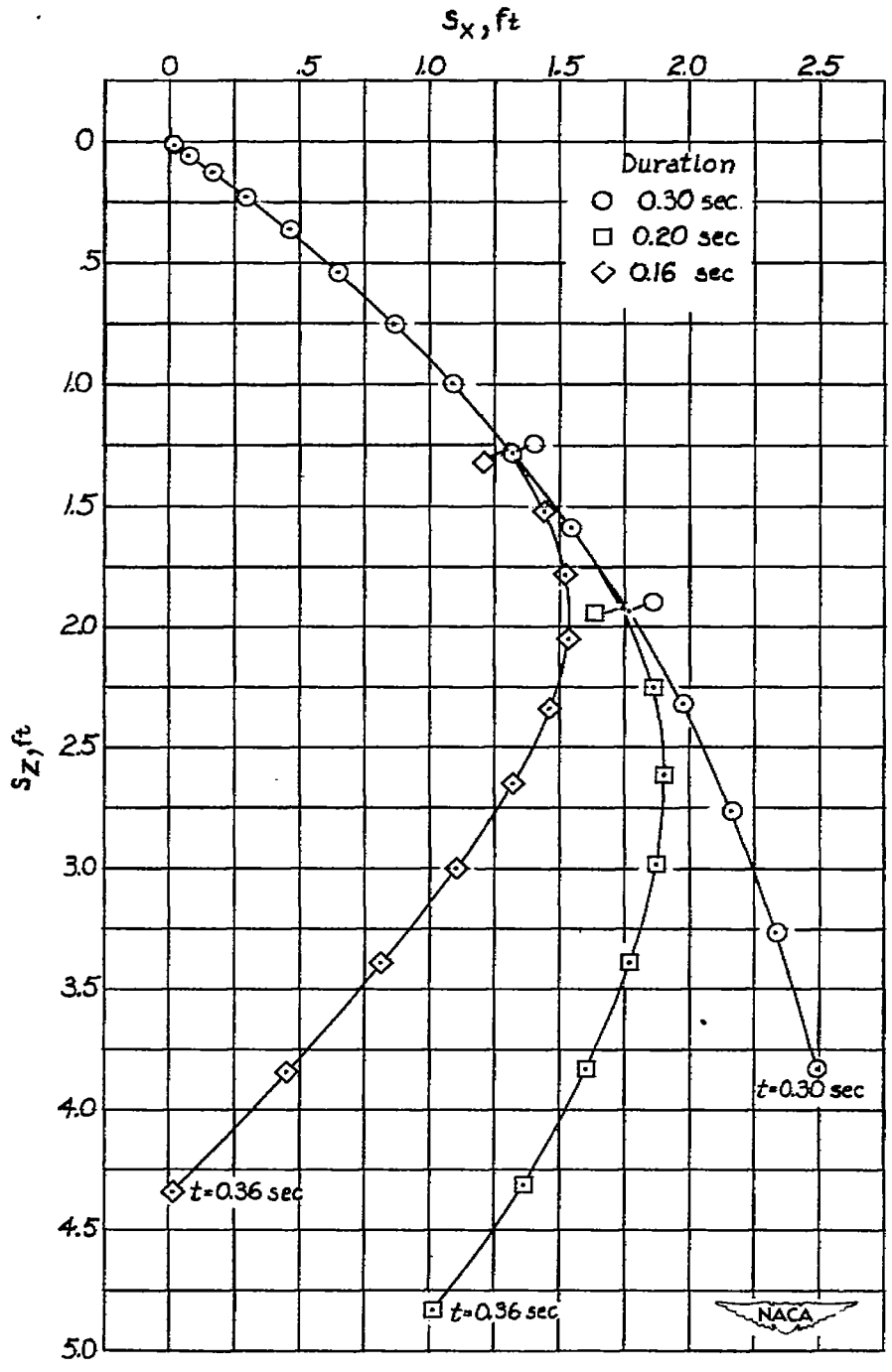

Figure 12.- Paths of the nose section jettisoned by a 4300-pound rocket thrust, assuming three different durations of rocket thrust. l = -0.05 foot; V_p = 800 feet per second.

[redacted]

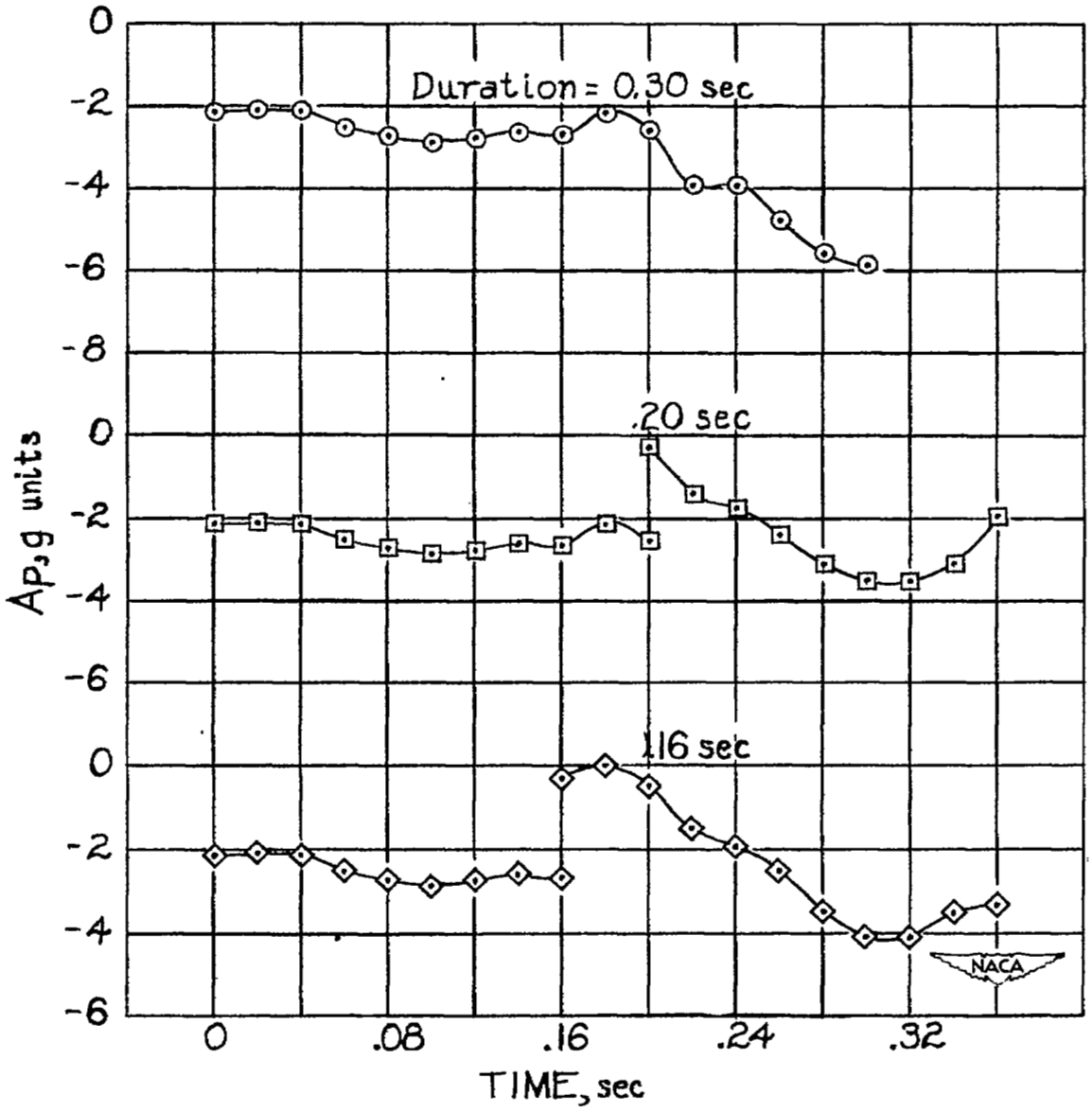

Figure 13.- Accelerations experienced by a pilot within a nose section jettisoned by a 4300-pound rocket thrust, assuming three different durations of rocket thrust. l = -0.05 foot; V_p = 800 feet per second.

[redacted]

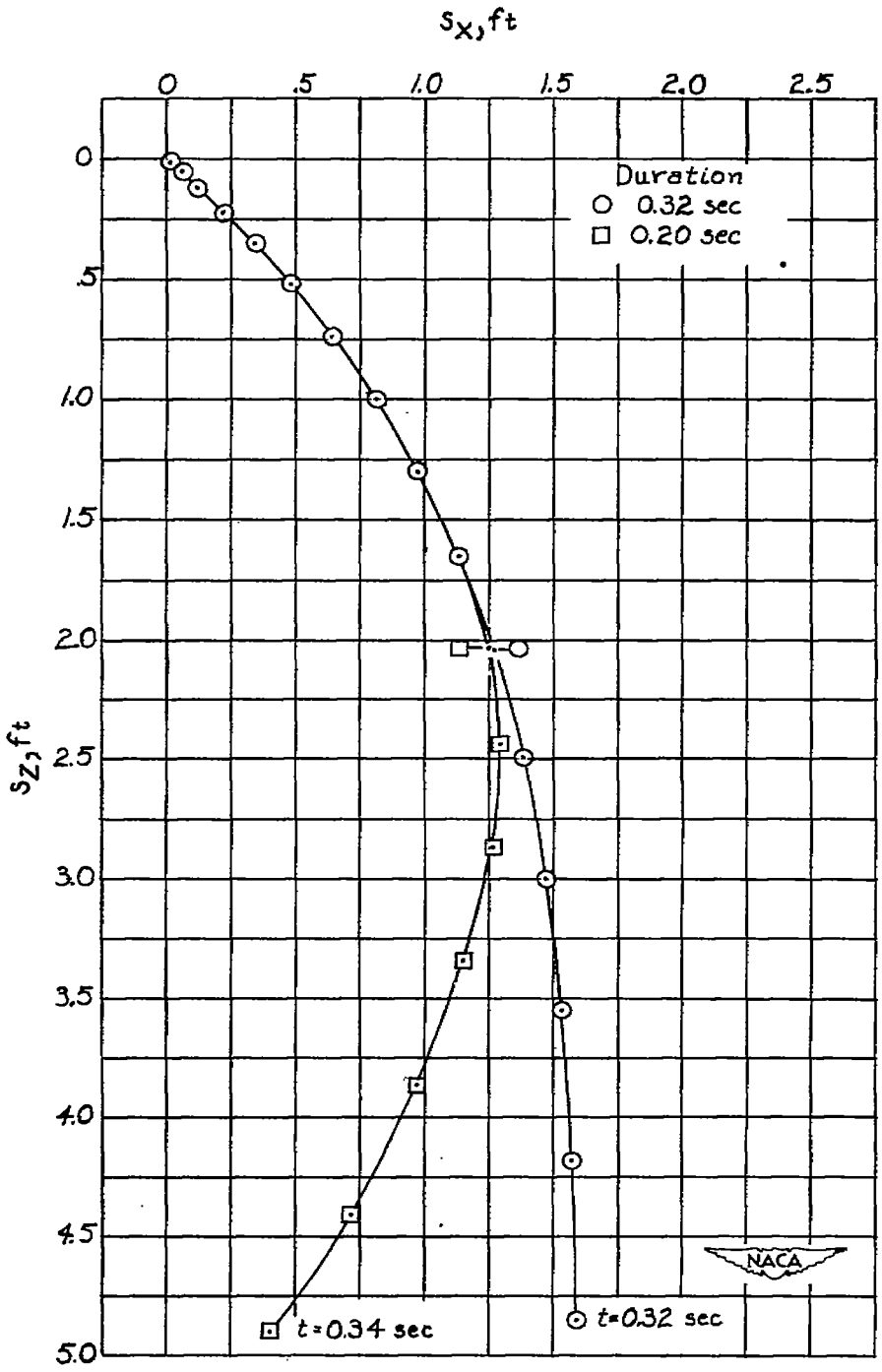

Figure 14.- Paths of the nose section jettisoned by a 3600-pound rocket thrust, assuming two different durations of rocket thrust. l = -0.10 foot; V_p = 800 feet per second.

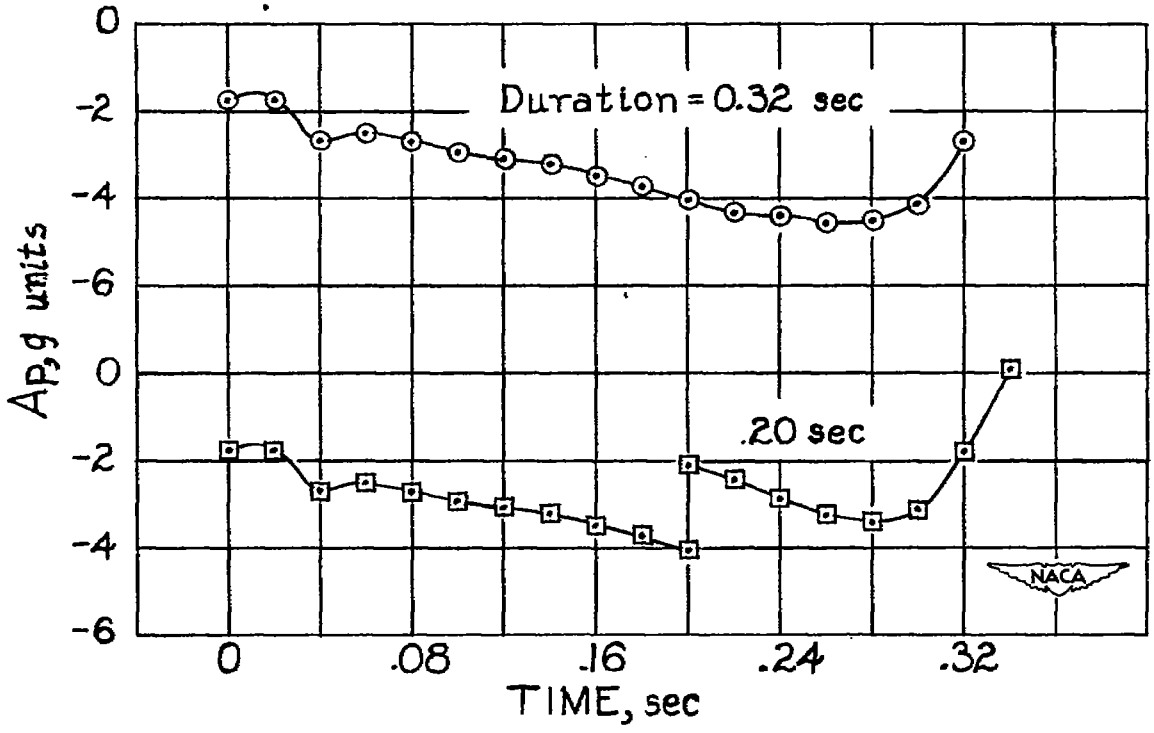

Figure 15.- Accelerations experienced by a pilot within a nose section jettisoned by a 3600-pound rocket thrust, assuming two different durations of rocket thrust. l = -0.10 foot; V_p = 800 feet per second.

[redacted]

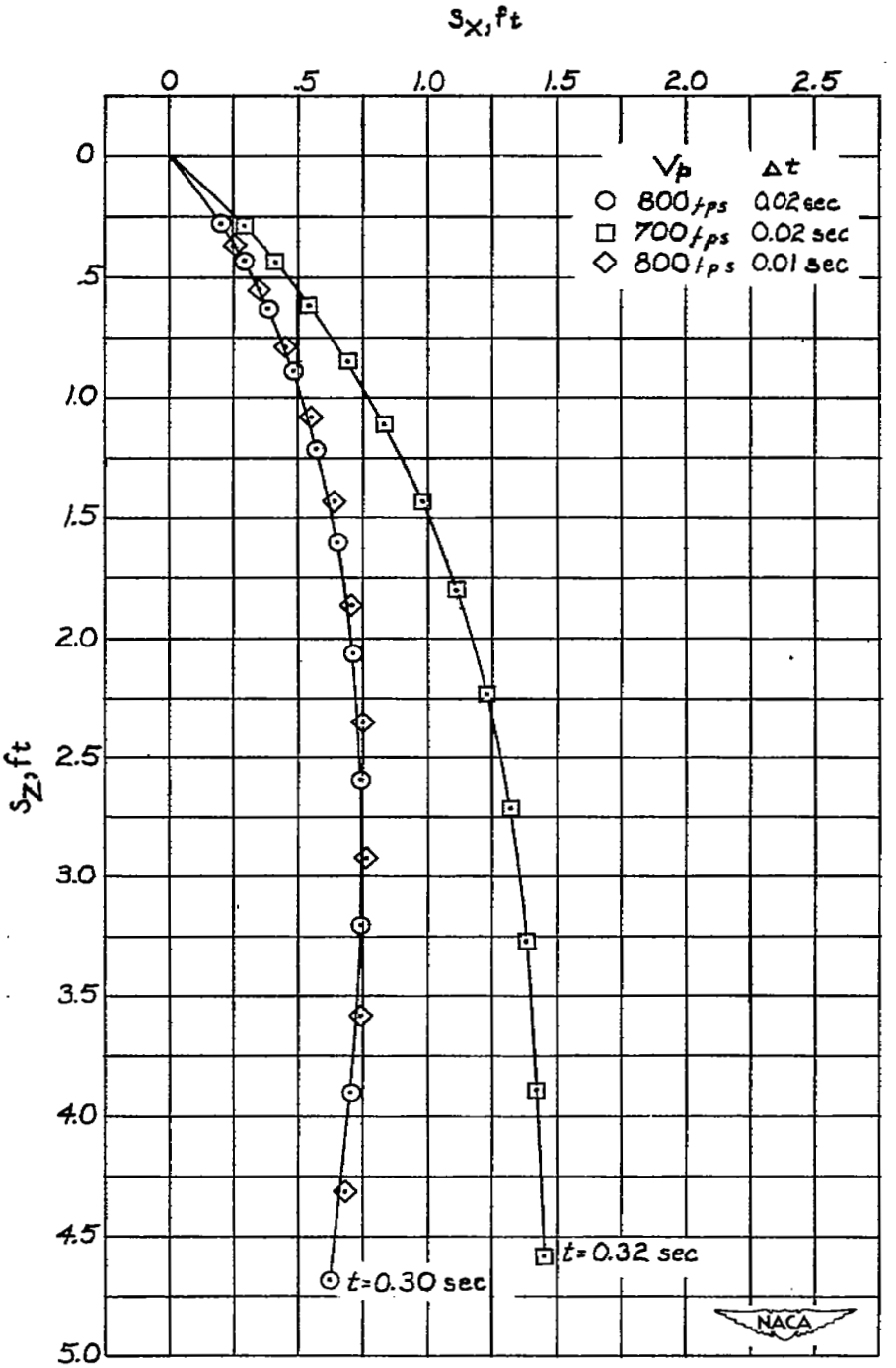

Figure 16.- Paths of the nose section jettisoned by a 2800-pound rocket thrust, assuming two different initial velocities. l = -0.20 foot.

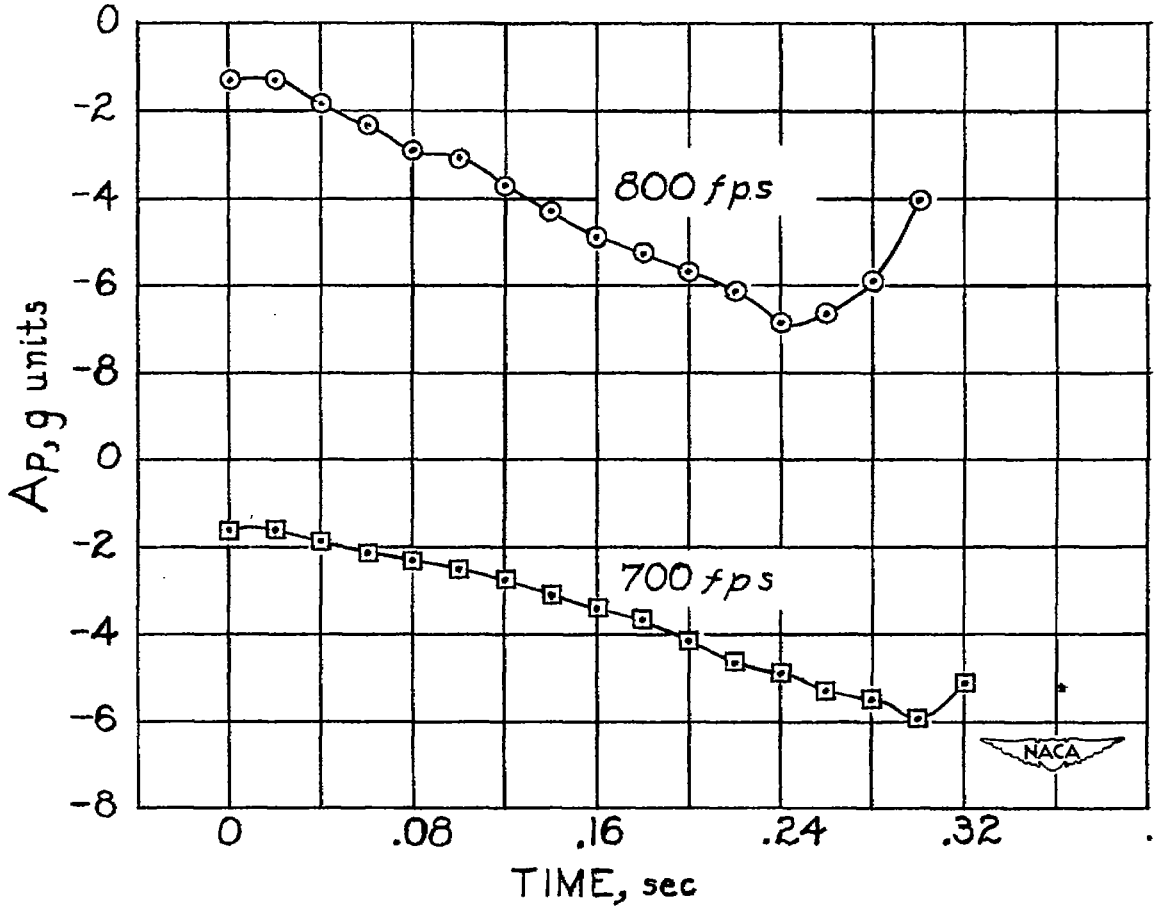

Figure 17.- Accelerations experienced by a pilot within a nose section jettisoned by a 2800-pound rocket thrust, assuming two different initial velocities. l = -0.20 foot.

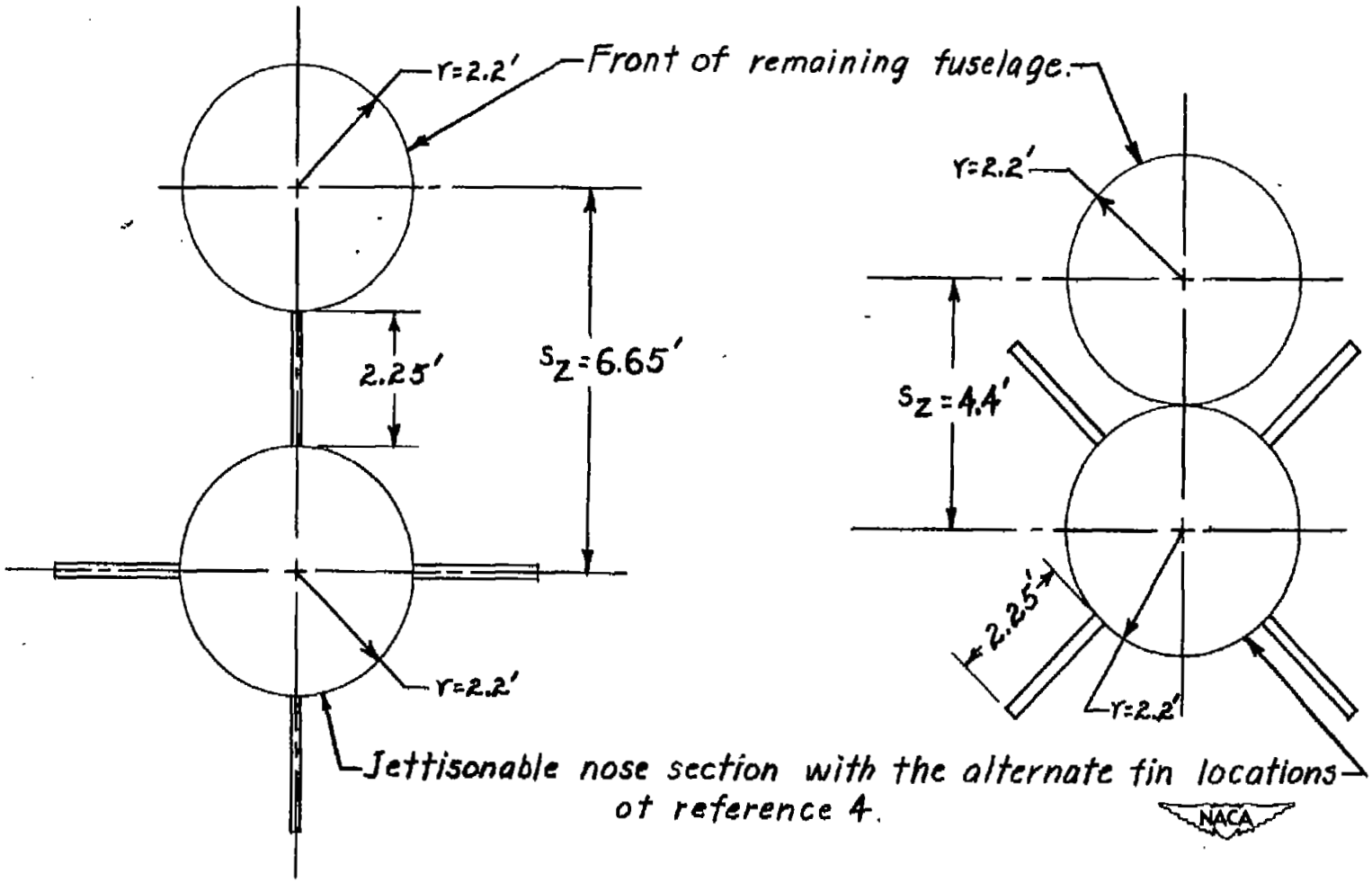

Figure 18.- Sketch showing the minimum value of s_Z necessary for clearing the rest of the airplane.